Proceedings of the 4th International Conference on Functional Materials and Civil Engineering
DOI: 10.54254/2755-2721/2026.38952

Investigation of the Physical Properties of High-Strength Nanocomposites

Qinze Liu

Beijing No. 4 High School, Beijing, China
13165317375@163.com

Abstract. In the context of today's era of an ever-accelerating production pace, people have placed extremely high demands on the quality and efficiency of mass production, and nanocomposites are undoubtedly an indispensable subject of discussion and a necessary product in this regard. As a highly necessary technological product of the new era, their production process is extremely tedious and complex, and the corresponding mass-production process cannot be readily realized. Existing preparation methods make it difficult to mass-produce nacre-mimetic composite films with highly ordered lamellae and a combination of high strength and toughness. The main reason is that engineering materials generally struggle to combine high strength and high toughness simultaneously, and the difficulty of mass-producing lightweight, high-performance materials is even greater. Therefore, how to make the production process of nanocomposites simpler and faster than existing approaches has become a very important issue.

Keywords: high strength, hardness, bioinspired nanocomposites

1. Introduction

1.1. Research background, application fields, prospects, value, and an overview of nanocomposites

Lightweight, high-toughness structural materials are a core demand in fields such as biomedicine and aerospace. Traditional single ceramics and polymer materials exhibit obvious shortcomings: pure ceramics are brittle and prone to fracture, while polymers lack sufficient stiffness, making it difficult for either to simultaneously meet load-bearing and impact-resistance requirements. Nanocomposites have therefore become the mainstream direction for resolving this contradiction. Nanocomposites use polymers or ceramics as the matrix, combined with nanofillers such as graphene and hydroxyapatite, and achieve synergistic performance through multi-scale hierarchical structures. By structural form, they can be divided into three major categories: lamellar-stacked nanocomposites, 3D-direct-written porous ceramic nanocomposites, and bioinspired hierarchical composites. Such materials combine the processing advantages of the matrix with the high-strength and highly conductive properties of the nanofillers; weak interfacial interactions such as hydrogen bonds and van der Waals forces can produce toughening effects such as crack deflection and

© 2026 The Authors. This is an open access article distributed under the terms of the Creative Commons Attribution License 4.0 (https://creativecommons.org/licenses/by/4.0/).

DOI: 10.54254/2755-2721/2026.38952

lamellar sliding, perfectly compensating for the mutual exclusivity of strength and toughness in traditional materials.

In terms of applications, hydroxyapatite direct-written porous nanocomposite scaffolds can be used in bone tissue engineering, with pore structures that accommodate cell proliferation; bioinspired lamellar graphene films are suitable for flexible conductive devices; and composites that mimic shell and bone structures can be used to fabricate lightweight protective components. From the perspective of development prospects, nanocomposites rely on 3D printing, layer-by-layer self-assembly, vacuum-assisted filtration, and other low-cost preparation processes, enabling precise control of the microstructure and balancing functionality and processability, with outstanding potential for industrialization. Their core value lies in breaking through the performance limits of traditional materials through the hierarchical arrangement of simple components: without developing entirely new chemical raw materials, they rely solely on microstructural design to substantially improve comprehensive properties such as stiffness, toughness, and electrical conductivity, providing brand-new material solutions for scenarios such as medical implants, lightweight load-bearing components, and flexible electronics.

1.2. Literature review

Existing studies have found that natural biological materials such as bone and nacre rely on multi-scale hierarchical structures to achieve a coexistence of strength and toughness through lamellar sliding and crack deflection, and that interfacial states and microscopic defects directly determine the mechanical performance of the material. Studies on direct-written ceramics have shown that the defect systems of microwires and scaffolds are not identical, and that relying solely on single-filament test data would severely underestimate the compressive resistance of scaffolds. Research on graphene composites has also confirmed that the nanoscale stacking form and interfacial thermodynamics simultaneously regulate the mechanical and electrical properties of the material [1]; currently, artificial hierarchical nanocomposites are mainly prepared by direct-written 3D printing, LBL layer-by-layer self-assembly, VAF vacuum-assisted filtration, and freeze-casting bioinspired replication, but each of these processes has obvious limitations: direct-written ceramic filaments inherently carry microporous defects, and the mechanical model needs to be recalibrated for different filament diameters; LBL preparation is cumbersome and difficult to mass-produce; VAF-produced films suffer from poorly ordered nanoplatelet arrangement and insufficient electrical conductivity. Meanwhile, existing bioinspired preparation methods find it difficult to replicate the complex multi-level gradient structures of natural materials, and most simulations remain at a single scale, lacking a unified mechanical prediction that can link microscopic fillers with macroscopic components. At this stage, many studies attempt to introduce machine learning to assist material structure design, so as to shorten the experimental cycle and screen the optimal microscopic arrangement schemes; however, this direction still lacks a mature cross-scale design framework and is difficult to apply directly to porous bioinspired ceramic scaffold systems [2].

1.3. Research status and development trends at home and abroad

International scholars have carried out extensive fundamental research on two typical systems: the first is direct-written porous ceramic scaffolds. Genet et al. established a micro-macro two-scale Weibull failure model, confirming that predicting strength based only on single-filament data yields extremely large deviations and requires calibration through scaffold experiments [3]; the second is bioinspired nanocomposites, for which multiple reviews have sorted out the toughening mechanisms

DOI: 10.54254/2755-2721/2026.38952

of natural hierarchical structures such as nacre and cuticle, and compared two graphene composite processes, layer-by-layer self-assembly (LBL) and vacuum-assisted filtration (VAF) [4], finding that the interfacial thermodynamic state determines the mechanical properties of the material while the lamellar stacking mode regulates the electrical conductivity. Domestic research mostly focuses on the optimization of material preparation processes, emphasizing the improvement of printing inks and the ratios of composite fillers; however, cross-scale mechanical prediction models and the large-scale preparation of bioinspired structures remain weak [5].

1.4. Research content and research objectives

This paper takes the nacre-mimetic nanocomposite (alumina nanoplatelets) as the research object, analyzes the physical strength of the nacre-mimetic nanocomposite formed by the material, and observes the effects of the microstructure on the stiffness, toughness, and strength of the material. The research objective is to summarize the structure-property relationships of nanocomposites, clarify the mechanical analysis methods, and provide a theoretical basis for subsequent research on nacre-mimetic nanocomposites.

2. Methods and materials

The experiment is divided into three parts: preparing the material green body, kneading and pressing into sheets, and drying and crystallization. The main purpose of the first part is to stir the green body until it is uniform, so as to avoid an uneven distribution of the final nanocomposite caused by insufficient stirring; after the first part, a viscoelastic substance is obtained. The main content of the second part is to knead the green body and then press it into a sheet, so as to ensure that the internal material is uniformly arranged and that the nanomolecular chains are uniform and oriented. The third part is grinding and crystallization: after the green body has been left to stand for a period of time, it is ground to facilitate the final testing of its physical properties.

Approximately 5.2 g of alumina nanoplatelets and 2.0 g of a 10% PVA solution were weighed using an analytical balance. First, the PVA solution was placed into a 25.0 mL beaker, and then 5.2 g of alumina nanoplatelets were added. A magnetic stir bar was placed into the beaker, and the beaker was positioned at the center of the magnetic stirring plate of the stirrer. The contents of the beaker were then stirred at a uniform speed of about 1.0 rev/s until uniformly mixed, which took about 1 hour. After removing the beaker from the magnetic stirring plate and confirming that the mixture was fully and uniformly stirred, two drops (approximately 0.2 mL) of borax test solution were added dropwise with a pipette. After stirring until fully mixed and the substance began to become strongly viscous, another two drops (approximately 0.2 mL) of borax test solution were added dropwise with the pipette, and stirring continued until no material adhered to the walls. The substance was then taken out with a glass rod, transferred to a plastic box, and the lid was closed to ensure a seal.

After the green body had been sealed and stored in the plastic box for about 12 h, it was taken out and placed on a clean glass plate with no foreign matter on its surface. The back of a Petri dish was used to knead the green body until it reached a length of about 10 cm, and it was then folded in half. This series of operations was repeated 50 times, ensuring that each fold after kneading was made along the crease from the previous operation, so as to keep as few bubbles as possible in the green body. The green body was then folded in half along the crease, and its dimensions were checked to ensure that it was not too wide or too thick for the pressing-hole size of the pressing machine, so as to avoid residue remaining on both sides after pressing due to excessive width or thickness, which would cause inconvenience in subsequent grinding. It was placed into the coarser of the three

DOI: 10.54254/2755-2721/2026.38952

pressing holes of different sizes in the pressing machine, and the handle was turned slowly at a uniform speed to control the pressing rate, so as to avoid non-uniform thickness caused by uneven speed. After pressing once in the coarser pressing hole (hole 1 in Figure 1), it was folded in half again along the crease and placed into the finer pressing hole (hole 2 in Figure 1) for another pressing; this operation was repeated ten times before this part of the procedure was completed. These operations ensured that the material inside the green body was uniformly arranged and that the nanomolecular chains were uniform and oriented.

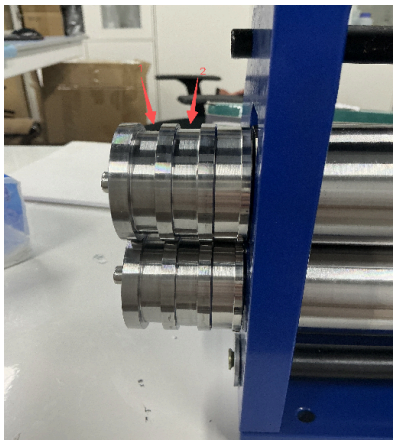


Figure 1. The three pressing holes of the pressing machine

After pressing, the material was folded in half along the crease, placed into the mold, and left to stand for about 36 hours. It was then taken out; if it had fully solidified, it was placed on the grinding disk for grinding. During grinding, the green body needed to be held with both hands, or moved up and down, to achieve higher grinding precision. During grinding, if the sandpaper became insufficiently rough due to prolonged use, it should be replaced with new sandpaper in time to ensure grinding efficiency and quality. The material first had to be roughly ground into a rectangular block, and after its shape was fixed, it was finely ground until the surface was free of uneven marks. Each face was ground for about 3-4 minutes at a rotation speed of about 50 rev/min. A rotation speed that was too high could lead to low grinding quality, leaving the material surface rough and uneven, whereas a rotation speed that was too low could lead to low grinding efficiency and an insignificant effect.

3. Results and analysis

After completing the operations in the experimental procedure section, mechanical performance tests needed to be carried out on the resulting material to obtain its bending strength. Before the mechanical tests, the length, width, and height of the material had to be measured for the subsequent calculation of the bending strength. A vernier caliper with a measuring range of 100.0 mm was used, and the measured length, width, and height were 19.8 mm, 2.90 mm, 2.64 mm, respectively. Half of its length (9.9 mm) was measured, and the midpoint was marked on the material for use in the subsequent mechanical performance tests.

The two ends of the nanocomposite were fixed to the two ends of the support frame of the three-point bending testing machine, to prevent additional displacement during the test that would make the data inaccurate. When placing the specimen, it was necessary to confirm that the midpoint marked before the test was at the center of the instrument. The blade part of the machine was

DOI: 10.54254/2755-2721/2026.38952

adjusted to move down until the blade body slightly contacted the surface of the nanocomposite. The equipment was then operated to move downward at a speed of 3 mm/min until the nanocomposite was completely broken, and the data displayed on the machine screen were collected, integrated, and used to plot the corresponding charts. The charts were analyzed to draw the final conclusion.

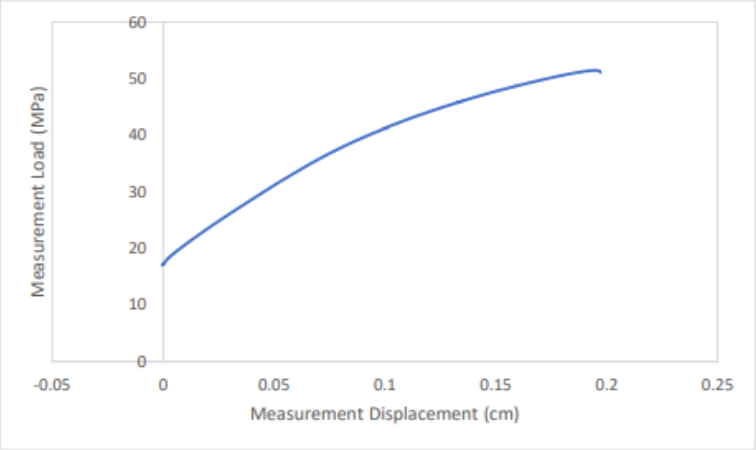


Figure 2. Measurement load-measurement displacement image of the nanocomposite

After organizing the data, the image was obtained (as shown in Figure 2), in which the vertical axis is Measurement Load (measurement load, in units of N), and the horizontal axis is Measurement Displacement (measurement displacement, in units of mm).

From Figure 2, we can see that the measurement load is positively correlated with the displacement, and the slope gradually decreases over time; these phenomena indicate that the bending strength of the material did not change significantly during the experiment.

According to the formula for bending strength, given that the length, width, and height of the specimen are 19.8 mm, 2.90 mm, 2.64 mm, respectively, the maximum load is 51.0050468444824 N, and the measurement displacement is 0.197174072265625 mm, according to the formula σ_f=3FL/3FL/(2bh²), the bending strength is approximately 0.75 MPa.

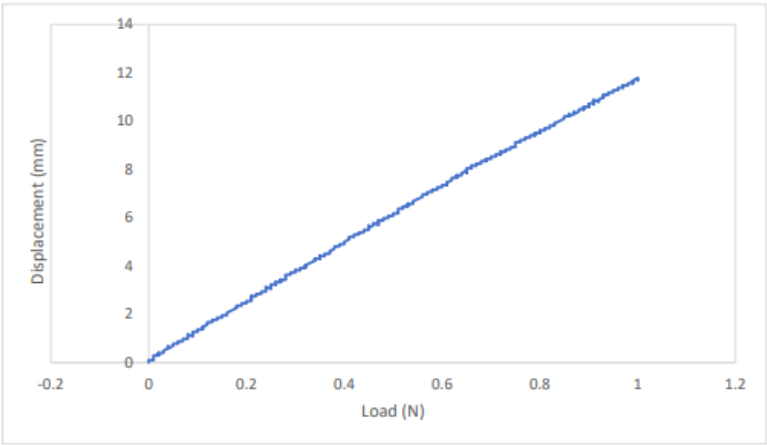


Figure 3. PVA colloid measurement load-measurement displacement image

According to Figure 3, the bending strength calculated for it is found to be far lower than that of the nanocomposite in Figure 2 (0.75 MPa). Analyzing the experimental data, we can conclude that

DOI: 10.54254/2755-2721/2026.38952

the strength of the nanocomposite is far greater than that of the PVA colloid.

After analyzing the experimental data and plotting the charts, a piece approximately 1.0 mm in length was cut from the end of a fractured nanocomposite specimen near the crack, for subsequent observation under the electron microscope.

Before observation, the sample material was cleaned and dried to ensure that it was free of moisture and surface impurities and that its morphology was stable. It was then attached to the sample stage with conductive tape and pressed firmly to prevent the sample from drifting under vacuum or the electron beam. The SEM specimen chamber was opened, the sample stage containing the material was placed inside, and the chamber door was closed tightly. The vacuum pump was started to evacuate the specimen chamber until it reached the vacuum level required by the instrument. Parameters such as the working current and scanning speed were adjusted, and the sample stage was moved manually to position the target observation region directly beneath the electron beam. Observation began after adjusting to a low magnification of 50x.

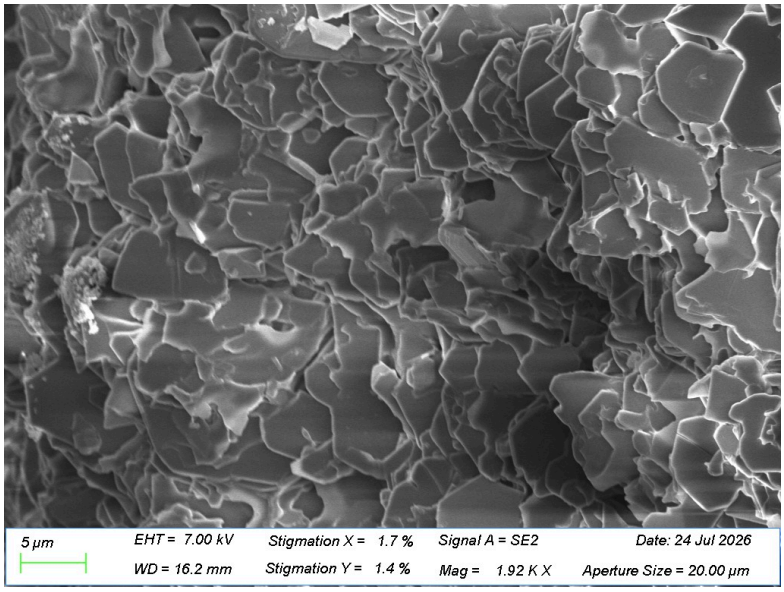


Figure 4. SEM image of the alumina nanocomposite

From Figure 4, we can see that the alumina nanoplatelets are distributed very densely. This phenomenon indicates that the physical strength of the resulting nanocomposite is very high, and its microstructure is not easily damaged, which also gives rise to its extremely high stability. From this, we conclude that the physical strength of a nanocomposite is positively correlated with its microscopic density: materials with a higher microscopic density exhibit higher physical strength. Moreover, we can also observe that the alumina nanoplatelets are arranged in a uniform and singly oriented distribution, and these phenomena indicate that the microstructures of most nanocomposites are uniformly oriented.

4. Conclusion and outlook

This paper aims to investigate the relationship between the physical strength of high-strength nanocomposites and their internal microstructure. Based on the support load and measurement displacement obtained by the three-point bending test and the microstructural image observed under the electron microscope (as shown in Figure 4), it can be concluded that the physical strength and stability of the nanocomposite with added alumina nanoplatelets far exceed those of ordinary PVA

DOI: 10.54254/2755-2721/2026.38952

colloid after crystallization. However, the experiment still has defects and limitations in certain aspects: the experiment was carried out using the single-variable method, but the selected materials were limited, including only the PVA colloid and the PVA colloid with added alumina nanoplatelets, without the addition of other nanomaterials; therefore, the influence on the experimental conclusions caused by differences in the microstructures of nanowire and nanoplatelet materials cannot be ruled out.

The conclusions drawn from this research can, in terms of materials physics, provide strong evidence of fundamental theory for future research on bioinspired nanocomposites. Future research on bioinspired nanocomposites will inevitably move toward the production of high-quality, high-strength nanocomposites, and future research directions will also focus more on methods for the mass production of high-strength bioinspired nanocomposites.

References

[1] Genet, M., Houmard, M., Eslava, S., et al. (2013). A two-scale Weibull approach to the failure of porous ceramic structures made by robocasting: Possibilities and limits. *Journal of the European Ceramic Society, 33*(4), 679-688.

[2] Nepal, D., Kang, S., Adstedt, K. M., et al. (2023). Hierarchically structured bioinspired nanocomposites. *Nature Materials, 22*(1), 18-35.

[3] Buehler, M. J., & Zhou, S. (2021). Bioinspired hierarchical composite design using machine learning: Simulation, additive manufacturing, and experiment. *Advanced Materials, 33*(29), 2101245.

[4] Zhu, J., Zhang, H., & Kotov, N. A. (2013). Thermodynamic and structural insights into nanocomposites engineering by comparing two materials assembly techniques for graphene. *ACS Nano, 7*(6), 4818-4829.

[5] Wegst, U. G. K., Bai, H., Saiz, E., et al. (2015). Bioinspired structural materials. *Nature Materials, 14*(1), 23-35.